LETTER

Particle robotics based on statistical mechanics of loosely coupled components

Shuguang Li[1,2,6]*, Richa Batra[2,6]*, David Brown[3], Hyun-Dong Chang[3], Nikhil Ranganathan[3], Chuck Hoberman[4,5], Daniela Rus[1] & Hod Lipson[2]*

Biological organisms achieve robust high-level behaviours by combining and coordinating stochastic low-level components[1–3]. By contrast, most current robotic systems comprise either monolithic mechanisms[4,5] or modular units with coordinated motions[6,7]. Such robots require explicit control of individual components to perform specific functions, and the failure of one component typically renders the entire robot inoperable. Here we demonstrate a robotic system whose overall behaviour can be successfully controlled by exploiting statistical mechanics phenomena. We achieve this by incorporating many loosely coupled 'particles', which are incapable of independent locomotion and do not possess individual identity or addressable position. In the proposed system, each particle is permitted to perform only uniform volumetric oscillations that are phase-modulated by a global signal. Despite the stochastic motion of the robot and lack of direct control of its individual components, we demonstrate physical robots composed of up to two dozen particles and simulated robots with up to 100,000 particles capable of robust locomotion, object transport and phototaxis (movement towards a light stimulus). Locomotion is maintained even when 20 per cent of the particles malfunction. These findings indicate that stochastic systems may offer an alternative approach to more complex and exacting robots via large-scale robust amorphous robotic systems that exhibit deterministic behaviour.

Many types of living cell can aggregate and migrate in a collective fashion, for example, during wound healing, morphogenesis and cancer metastasis[8–10]. A variety of bio-inspired modular or swarm robotic systems have been developed in an attempt to emulate such behaviours through coordinated locomotion, cooperative transport and self-assembly[6,11].

However, most robotic systems today either require some degree of centralized control[7] or rely on deterministic behaviour, limiting the capabilities and scalability of the entire system[11–14]. Most other modular robotic systems have limited flexibility of permitted configurations—such as our own Crystal robots[15] and Molecubes[6], which are constrained to lattice structures. More amorphous systems, such as Slimebots[16], amoeboids[17], robotic stem cells[18] or digital hormone models[19], typically involve modules with a variety of design complexities and multiple degrees of freedom that would be challenging to scale to large numbers and small sizes.

Here, we study an alternative approach that aims to reduce these constraints to a bare minimum to potentially afford better scalability and robustness. We refer to this minimalistic approach as particle robotics because each element has no unique identity. Inspired by the collective migration phenomena in cell biology[20–22], particle robots are designed as amorphous systems comprising numerous loosely coupled simple 'particles'. Although each particle lacks a unique identity (that is, it cannot be addressed individually) and is incapable of controlled locomotion or direct communication with other specific particles, the cohort can nonetheless display aggregate and robust behaviours.

The lack of independent locomotion for each particle could also help us to better understand the role of collective mechanics in emergent swarm locomotion. We are also inspired by statistical physics
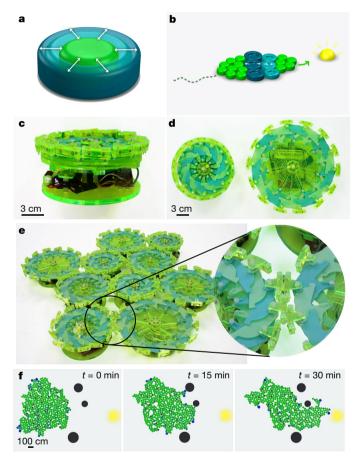

Fig. 1 | A particle robot is composed of many loosely coupled individual 'particles'. a, Each particle is only capable of oscillating along its radius. **b**, Multiple particles are loosely coupled to form an agglomerated organism, which is moving towards a light source in the figure. By oscillating in relation to their distance from the light source, the particles' radii vary in an undulating fashion at a single frequency. **c**, An oblique view of a disk-shaped particle. **d**, The particles in contracted (left) and expanded (right) view, with diameters of 15.5 cm and 23.5 cm, respectively. **e**, The particles are loosely coupled using dangling magnets. **f**, When particles oscillate in a particular pattern, a global behaviour emerges, including phototaxis and obstacle avoidance. The colour of oscillating particles ranges from green (minimum radius) to blue (maximum radius), whereas dead particles are depicted in grey. The black circles represent obstacles and the stimulus is denoted by a yellow circle.

[1]Computer Science and Artificial Intelligence Laboratory, Massachusetts Institute of Technology, Cambridge, MA, USA. [2]Creative Machines Laboratory, Mechanical Engineering Department, Columbia University, New York, NY, USA. [3]School of Mechanical and Aerospace Engineering, Cornell University, Ithaca, NY, USA. [4]Graduate School of Design, Harvard University, Cambridge, MA, USA. [5]Wyss Institute for Biologically Inspired Engineering, Harvard University, Cambridge, MA, USA. [6]These authors contributed equally: Shuguang Li, Richa Batra. *e-mail: lisg@csail.mit.edu; richa.batra@columbia.edu; hod.lipson@columbia.edu
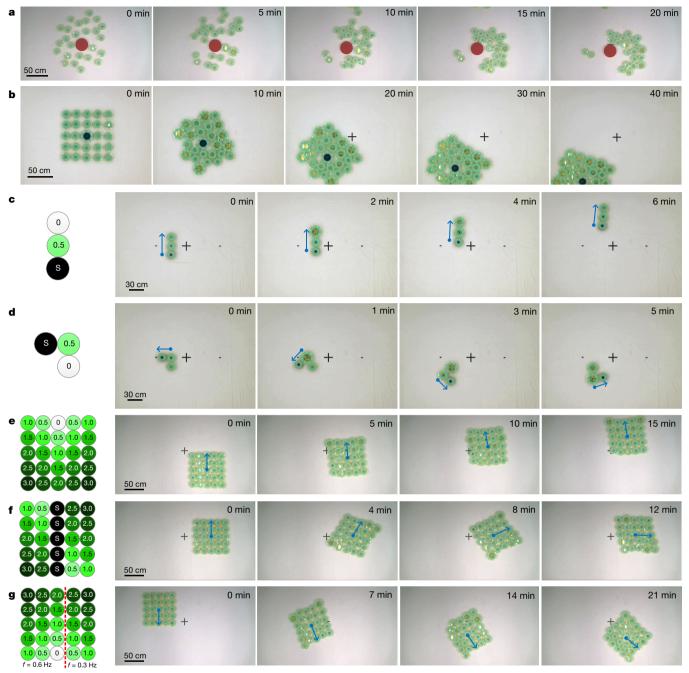
Fig. 2 | Locomotion methodology. a, Particles with randomly assigned phase offsets are initially scattered around an obstacle and begin to cluster over time. **b**, Particles with randomly assigned phase offsets are placed in a grid with an object intended for transport located in the centre, demonstrating locomotion in an unpredictable direction. **c**, Three particles in a row with sequentially assigned phase offsets exhibit forward locomotion. **d**, Reorienting the three particles into an asymmetric configuration produces turning with a consistent radius of curvature. **e**, A grid of particles exhibits forward locomotion when assigned a phase offset relative to their respective distances from the top-central particle. **f**, A grid of particles incorporating a column of inactive particles in the middle, assigned a mirrored phase offset pattern, turns. **g**, A grid of particles with a phase offset defined asymmetrically produces translation and rotation. The assigned phase offsets are shown in the left columns of **c–g**. The number on each particle represents its phase delay (in units of π, half cycle), whereas 'S' indicates that the particle is inactive, or dead, and does not oscillate.

phenomena, where global thermodynamic effects can be modelled and controlled without tracking each particle in a gas.

This work is motivated by the need for greater scalability in modular robots, which can be attained when robotic systems are composed only of such loosely coupled particles without individual identity. It is also envisaged that this design is more robust in case of malfunctioning or death of several (or even many) particles.

The hypothesized scalability is due to several factors, the first of which relates to the fact that individual particles are not required to have independent locomotive ability, as in most swarm robotic systems, where each module requires more complex degrees of freedom. Simple particles are easier to manufacture and maintain in large numbers. This design simplicity is particularly valuable at the microscale, where individual locomotion is difficult to create and control[23–25]. Second, by eliminating individual identity and addressability, communication challenges typically associated with very large swarms can be eliminated. Stochastic organization also removes any single point of failure typically characterizing deterministic modular and monolithic
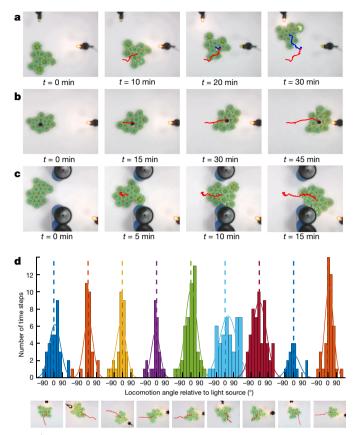
Fig. 3 | Deterministic behaviour emerges from collective stochastic motion. a, When particles oscillate in a phase proportional to their level of illumination, the agglomeration moves towards the light source, demonstrating phototaxis. **b**, **c**, The organism can cooperatively transport an object (**b**) and manoeuvre around obstacles (**c**). **d**, Random configurations of 9–10 particles with different light-source locations were tested. The angle of motion of the particle robot from its centroid to the light source was measured at 30-s intervals and is plotted in a shifted fashion, with the Gaussian distribution curve (solid) and the mean angle (dashed) overlaid. An image of each experiment in its final configuration with its centroid traced is displayed underneath each graph.

robots. A single point of failure requires specialized repair and recovery routines. Third, the particles are loosely coupled, which allows more complex behaviours in unfamiliar environments, such as object transport or obstacle avoidance. Moreover, a particle robot can be generated, self-healed or grown in size and capacity simply by pouring more particles that couple together.

To investigate this concept, we designed a robot comprising many disk-shaped particles. To maintain the simplicity hypothesis, each particle has only a single degree of freedom and is solely capable of radial expansion and contraction (Fig. 1). The particles can actively respond to their local environment and communicate with each other through non-specific communication (broadcast only). In addition, each particle is 'sticky' to ensure that it adheres to adjacent particles with an attraction force greater than its static friction, yet it remains loose enough so that passive connectivity can be broken and re-established spontaneously (Fig. 1e).

Because each particle can only expand and contract, it will remain stationary when in isolation. Even a pair of connected particles will simply oscillate, and groups of particles placed in close contact will at most perform a random walk as an aggregate.

Interesting behaviour emerges, however, when particles are programmed to behave in systematic patterns. For example, when particles offset the phase of their oscillation in response to some environmental signal gradient, the individual stochasticity is channelled into systematic and robust collective locomotion towards the signal source

(Fig. 1b). This movement occurs even though no particle is capable of individual locomotion or coordination with other individual particles. Furthermore, elimination or malfunctioning of some of the particles in the aggregate would result in gradual (proportionate) performance degradation. Owing to these characteristics, it is envisaged that this robot architecture may be suitable for applications requiring economy of scale, adaptability and robustness (Fig. 1f, Supplementary Video 1).

The coordinated movement of a particle robot comprising many particles is achieved by modifying the phase of each particle's expansion–contraction cycle with respect to its relative position. Initially, various configurations with particles modulating at random phase offsets were tested to observe the locomotion characteristics and formation behaviours of the collective. When initialized in a scattered configuration, the cluster of particles tends to disintegrate into smaller amorphous groups, as shown in Fig. 2a. In Fig. 2b, particles are placed in a grid around an object intended for transport and then modulated at random phase offsets, which results in an unpredictable, Brownian-like movement of the entire system. However, when the phase is modulated in proportion to some gradient, periodic waves of oscillation emerge across the system. These waves result in incremental shifts in the centre of mass of the system, yielding a net forward motion.

To understand the effects of various wave propagation schemes, different particle configurations were tested with respect to the assigned phase offsets. The dynamics of a coordinated expansion–contraction strategy were studied using small chains of particles, demonstrating forward motion (Fig. 2c). Moreover, by manipulating the chain configuration, turning with a consistent radius of curvature was achieved (Fig. 2d). In addition, lattice configurations with different expansion and contraction schemes (Fig. 2e–g) were employed to study the resultant motion (Supplementary Video 3).

It should be noted that similar coordinated push–pull locomotion strategies have been used to operate traditional, lattice-type modular architectures, successfully demonstrating multi-robot locomotion with both chain-shaped linear configurations and two-dimensional array configurations[26–28]. However, the proposed design does not require a lattice structure, which in fact creates unnecessary constraints.

To achieve autonomous locomotion directed by an external stimulus, a simple distributed algorithm inspired by collective cell migration phenomena in biology was developed (Supplementary Information section S5). This algorithm stipulates that each particle's phase offset is proportional to the intensity of the signal that it is sensing. This simple strategy eliminates the need for any kind of explicit coordination among the particles. The proposed methods were implemented using robot particles and an environmental signal to successfully perform locomotion, object transport and obstacle avoidance (Fig. 3a–c, Supplementary Video 4). To verify the phototaxis behaviour, nine arbitrary configurations of the particle robot comprising either nine or ten particles were tested (Fig. 3d) while varying the light source location to eliminate any potential directional bias of the experimental setup (due to possible directional friction or tilt, for example).

In addition to the experimental verification of the particle robot performance, a simulation environment was developed based on the particle's physical characteristics. To test the robustness of the design, simulations with a fixed percentage of randomly chosen inactive, or dead, particles were performed (Fig. 4). Ten randomly initialized configurations were created for each system comprising 10, 100, 1,000 and 10,000 particles. The simulations were run for approximately 14.4 million loops, or 1,200 expansion–contraction cycles, with different percentages of dead particles, and the average centroid speed was measured (Fig. 4a, Supplementary Video 6). These simulation findings revealed that the system speed declines as the percentage of dead particles increases. Nonetheless, with 20% dead particles, the system was still able to move at 48%–60% of its fully functioning speed, illustrating the robustness of the particle robot framework to individual component failures (Supplementary Information section S8).

The analysis results also indicate that the particle robot speed is dependent on the effective wavelength of the phase offset response,
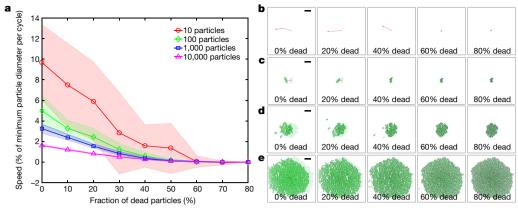
Fig. 4 | Statistical analysis of the behaviour of the particle robot shows that its motion is scalable and robust. a, The speed of motion (expressed as the percentage of the minimum particle diameter per cycle) towards the light source decays as the percentage of dead (malfunctioning) particles increases. For each combination of number of particles and percentage of dead particles, ten random configurations were simulated and analysed. Scaling the number of particles also reduces the variance in the speed, as indicated by the standard deviation (shaded area). **b–e**, Simulation results for random configurations of 10 particles (**b**), 100 particles (**c**), 1,000 particles (**d**) and 10,000 particles (**e**) with varying percentages of dead particles are shown after 1.44 million cycles or 2 h. The active particle colour ranges from green (at the minimum radius) to blue (at the maximum radius), whereas dead particles are shown in grey. The initial configuration is superimposed in each panel with transparency, with the centroid trace shown in red. The black scale bar represents 300 cm.

defined as the length at which the phase offset begins to repeat. As the particle robot size increases, multiple waves of oscillation can be observed across the system, whereby the average speed decreases proportionally. In addition, the variance decreases considerably as the number of particles in the system increases, and the robot's speed becomes predictable. In Fig. 4b–e, a random configuration for each particle robot size is depicted and the effects of the number of particles and percentage of dead particles on the motion can be observed. Although the simulations, which are modelled on the physical particles, suggest that there is a degradation of locomotion speed with an increase in the number of particles, we anticipate that physical realizations of particle robots with thousands of particles will be most effective with microscale particles. For particles of that size, surface tension, electric charge or chemical bonds could be used as the coupling mechanism, and the particle behaviour may be best modulated by an electric, magnetic or photonic field that can oscillate at higher frequencies. For example, recent research demonstrating spatiotemporal oscillations of colloidal swarms[29,30] provides strong evidence that such methods of mechanical adhesion are possible. However, the control and feasibility of consistent coupling forces between microscale robots are an additional challenge and would still need to be validated in the future. Furthermore, because the robot has no unique particles, it would be possible to increase its size by incorporating additional particles into the configuration. Similarly, the robot has the potential to grow by annexing stray particles in the environment or from other robots—essentially 'metabolizing' other robots.

There are, of course, many limitations to the proposed concept that would render it unsuitable for certain applications; tasks such as directed self-assembly and self-organization into complex pre-specified geometries would be difficult given the stochastic nature of the group and unconstrained placement or coupling of the particles. Furthermore, here the concept was demonstrated in two dimensions only, whereas a three-dimensional design would arguably be able to achieve more versatile manoeuvres and functions, such as lifting objects. In addition, the proposed concept needs to be optimized in terms of weight, size, speed and power efficiency. Here, we validated our concept using a group of 25 physical robots, with each particle having a diameter of approximately 15 cm. It would also be valuable to validate our concept experimentally on a large-scale swarm robotic system (more than 1,000 units) composed of much smaller robotic particles (at the microscale).

It should be noted that in the simulations, we observe clusters of particles detach and create splinter groups, particularly when there are 1,000 particles or more. These groups may later be annexed by the concentration of particles or continue to move at a different speed.

This separation may be due to the particle placement algorithm and the sparse initial configuration, or this behaviour is more probably a consequence of the particle parameters fitted to model the physical prototype, such as mass or attraction. There may be an optimal number of particles or configuration for a particle robot composed of such particles. We intend to explore this further using a simulation environment and to study the relationships between the particle parameters and the particle robots' performance.

Nonetheless, as was demonstrated in this work, particle robots appear to exhibit scalable control and robustness not seen in conventional robotic architectures, including traditional (deterministic) modular robots, where often the destruction of even a single component would typically result in catastrophic failure. This characteristic makes particle robotics a potentially viable option for the rapidly developing fields of micro- and nanoscale robotics, where consistent and deterministic mechanical performance is typically difficult to control because of the large numbers of components, which cannot be addressed individually. Finally, the view of robots as statistical, rather than deterministic, machines can offer new insight into the control of biological systems comprising billions of cells.

Online content

Any methods, additional references, Nature Research reporting summaries, source data, statements of data availability and associated accession codes are available at https://doi.org/10.1038/s41586-019-1022-9.

1. Rørth, P. Collective guidance of collective cell migration. *Trends Cell Biol.* **17**, 575–579 (2007).
2. Haeger, A., Wolf, K., Zegers, M. M. & Friedl, P. Collective cell migration: guidance principles and hierarchies. *Trends Cell Biol.* **25**, 556–566 (2015).
3. Tambe, D. T. et al. Collective cell guidance by cooperative intercellular forces. *Nat. Mater.* **10**, 469–475 (2011).
4. Felton, S., Tolley, M., Demaine, E., Rus, D. & Wood, R. A method for building self-folding machines. *Science* **345**, 644–646 (2014).
5. Wehner, M. et al. An integrated design and fabrication strategy for entirely soft, autonomous robots. *Nature* **536**, 451–455 (2016).
6. Zykov, V., Mytilinaios, E., Adams, B. & Lipson, H. Robotics: self-reproducing machines. *Nature* **435**, 163–164 (2005).
7. Rubenstein, M., Cornejo, A. & Nagpal, R. Programmable self-assembly in a thousand-robot swarm. *Science* **345**, 795–799 (2014).
8. Friedl, P. & Gilmour, D. Collective cell migration in morphogenesis, regeneration and cancer. *Nat. Rev. Mol. Cell Biol.* **10**, 445–457 (2009).
9. Weijer, C. J. Collective cell migration in development. *J. Cell Sci.* **122**, 3215–3223 (2009).

10. Méhes, E. & Vicsek, T. Collective motion of cells: from experiments to models. *Integr. Biol.* **6**, 831–854 (2014).
11. Chen, J., Gauci, M., Li, W., Kolling, A. & Gross, R. Occlusion-based cooperative transport with a swarm of miniature mobile robots. *IEEE Trans. Robot.* **31**, 307–321 (2015).
12. Butler, Z. & Rus, D. L. Distributed planning and control for modular robots with modules. *Int. J. Rob. Res.* **22**, 699–715 (2000).
13. Gross, R., Bonani, M., Mondada, F. & Dorigo, M. Autonomous self-assembly in swarm-bots. *IEEE Trans. Robot.* **22**, 1115–1130 (2006).
14. Yim, M. et al. Modular self-reconfigurable robot systems. *IEEE Robot. Autom. Mag.* **14**, 43–52 (2007).
15. Rus, D. & Vona, M. Crystalline robots: self-reconfiguration with compressible unit modules. *Auton. Robots* **10**, 107–124 (2001).
16. Shimizu, M., Ishiguro, A. & Kawakatsu, T. Slimebot: a modular robot that exploits emergent phenomena. In *Proc. 2005 IEEE International Conference on Robotics and Automation* 2982–2987 (IEEE, 2005).
17. Umedachi, T., Horikiri, S., Kobayashi, R. & Ishiguro, A. Enhancing adaptability of amoeboid robot by synergetically coupling two decentralized controllers inspired by true slime mold. *Adapt. Behav.* **23**, 109–121 (2015).
18. Rubenstein, M., Sai, Y., Chuong, C. M. & Shen, W. M. Regenerative patterning in Swarm Robots: mutual benefits of research in robotics and stem cell biology. *Int. J. Dev. Biol.* **53**, 869–881 (2009).
19. Shen, W.-M., Will, P., Galstyan, A. & Chuong, C.-M. Hormone-inspired self-organization and distributed control of robotic swarms. *Auton. Robots* **17**, 93–105 (2004).
20. Camley, B. A. & Rappel, W.-J. Physical models of collective cell motility: from cell to tissue. *J. Phys. D Appl. Phys.* **50**, 113002 (2017).
21. Ellison, D. et al. Cell–cell communication enhances the capacity of cell ensembles to sense shallow gradients during morphogenesis. *Proc. Natl Acad. Sci. USA* **113**, E679–E688 (2016).
22. Mugler, A., Levchenko, A. & Nemenman, I. Limits to the precision of gradient sensing with spatial communication and temporal integration. *Proc. Natl Acad. Sci. USA* **113**, E689–E695 (2016).
23. Zhang, L., Petit, T., Peyer, K. E. & Nelson, B. J. Targeted cargo delivery using a rotating nickel nanowire. *Nanomed. Nanotechnol.* **8**, 1074–1080 (2012).
24. Sitti, M. Voyage of the microrobots. *Nature* **458**, 1121–1122 (2009).
25. Hu, W., Lum, G. Z., Mastrangeli, M. & Sitti, M. Small-scale soft-bodied robot with multimodal locomotion. *Nature* **554**, 81–85 (2018).
26. Butler, Z. & Rus, D. Distributed planning and control for modular robots with unit-compressible modules. *Int. J. Robot. Res.* **22**, 699–715 (2003).
27. Yu, C. H., Werfel, J. & Nagpal, R. Coordinating collective locomotion in an amorphous modular robot. In *Proc. IEEE Int. Conf. Robot. Autom.* 2777–2784 (IEEE, 2010).
28. Vergara, A., Lau, Y., Mendoza-Garcia, R.-F. & Zagal, J. C. Soft modular robotic cubes: toward replicating morphogenetic movements of the embryo. *PLoS One* **12**, e0169179 (2017).
29. Altemose, A. et al. Chemically controlled spatiotemporal oscillations of colloidal assemblies. *Angew. Chem. Int. Ed.* **56**, 7817–7821 (2017).
30. Wang, B. et al. Reconfigurable swarms of ferromagnetic colloids for enhanced local hyperthermia. *Adv. Funct. Mater.* **28**, 1705701 (2018).

Author contributions H.L., S.L. and R.B. proposed the research; S.L., C.H. and H.L. designed the robots; S.L., H.L. and D.R. designed the control algorithms; S.L., D.B. and H.-D.C. fabricated the robots and conducted the physical experiments; R.B., S.L. and N.R. developed the simulations; R.B. performed the numerical experiments; R.B., S.L. and H.L. analysed the data and wrote the paper; all authors provided feedback.

Competing interests The authors declare no competing interests.

Additional information
Supplementary information is available for this paper at https://doi.org/10.1038/s41586-019-1022-9.
Reprints and permissions information is available at http://www.nature.com/reprints.
Correspondence and requests for materials should be addressed to S.L. or R.B. or H.L.
Publisher's note: Springer Nature remains neutral with regard to jurisdictional claims in published maps and institutional affiliations.

METHODS

Robot particle design. The proposed particle design consists of a cylindrical base, which houses the power, actuation, control, sensor and communication components (Fig. 1c). A modified Hoberman flight ring is mounted to the top, and a transmission mechanism translates the motor rotation into continuous radial expansion and contraction of the ring. Each particle has a weight of 576 g, a height of 7 cm and a diameter that can range from 15.5 cm to 23.5 cm (Fig. 1d). Additional information about the particle design and construction is available in Supplementary Information section S1.

A key practical challenge that had to be overcome when designing the particles pertained to the need to achieve loose temporary passive particle adhesion so that the particles move as a cohesive and mutable unit. Conventional approaches, such as Velcro, sticky tape or rigid magnets, were not suitable for this purpose, because they were either too inflexible or too weak. Thus, an appropriate passive-adhesion mechanism was developed specifically for this work, using a series of weak magnets mounted on flexible protrusions from the surface of each particle. The outer ring perimeter was fitted with fourteen flexible T-shaped compartments, each of which contained two magnetic spheres of 5 mm diameter (Fig. 1e). This arrangement ensures that when a particle comes into contact with a nearby particle, they adhere to one another owing to the flexible magnetic attraction of the outer edges of the oscillating rings. The flexibility of the protrusion permits the particles to remain in contact even as their diameters or positions change, enabling dense multi-particle agglomerations capable of directed locomotion (see Supplementary Video 2).

Control algorithms for autonomous locomotion. The algorithm can be implemented without resorting to individual particle-to-particle communication. The simplest approach involves translating the input signal to a phase offset directly using a static formula or a lookup table. A second, more adaptive approach requires each particle to broadcast the light intensity value that it is measuring. Each particle receives the values broadcasted by other particles and interpolates its phase offset. Alternatively, each particle can record only the number of received intensities that are greater than its own and determine its relative position accordingly. It is also feasible to adopt more sophisticated approaches based on statistical learning, which might yield slightly better performance, but are not strictly required (see Supplementary Information sections S2–S5). Irrespective of the method used, all particles must have a synchronized clock, which can be achieved by adopting distributed clocks[31]. The experiments performed as a part of this investigation were sufficiently short to render clock drift negligible.

Physical experiment setup and data analysis. In a series of phototaxis experiments, a desk lamp with a yellow light bulb, placed about 1 m away from the particle robot, served as the external stimulus signal source. The particles were manually placed in an arbitrary orientation, with each particle in contact with at least two other particles. The orientations of the coupled particles and the light source were varied to reduce bias. Using the interpolation approach outlined above, each particle determined its relative position in the pack. These steps were repeated at approximately 2–5-min intervals to update each particle's intensity reading and reset its motion phase offset on the basis of its current position with respect to the system and stimuli. We used a central computer to broadcast a synchronization message to the particles to initiate the update. Clock drift between these synchronization events was negligible. There are many biologically inspired distributed synchronization algorithms[31–35] that could be used for this purpose in future work. It should be noted that the overhead lights, which greatly enhanced the video quality and resolution of the experiments, were turned off during the phase update interval to avoid diluting the stimulus signal. These segments were typically cut from the experiment recording to reduce the length and file size.

Videos of the experiments were taken from above, and subsequent data processing allowed us to track the particle robot centroid position and determine whether movement in the desired direction was statistically significant (see Supplementary Information section S6). To compare the motions achieved in different experimental arrangements, the image coordinates were transformed so that the particle robot centroid in the first frame defined the coordinate system origin, whereas the light source centroid defined a point on the positive y axis. As the particle robots moved, the change in the centroid position in this coordinate system was recorded at 30-s intervals. It was imperative to consider the change in position over longer time

segments, instead of recording the centroid movement over 1-s intervals, given the undulating behaviour of the amorphous system.

A right-sided t-test for the motion of the centroid in the y direction revealed that the locomotion towards the light was significant at >99% confidence level. In addition, the centroid data collected at 30-s intervals were examined to determine the angle of motion with respect to the light source. The results pertaining to each experiment are plotted in Fig. 3d, above the image of the corresponding experiment. Although some experiments were performed over a longer time, producing larger datasets of motion at 30-s intervals, they can all be described by a Gaussian distribution centred at approximately 0° with respect to the light source direction.

Simulation environment. The friction, attraction and expansion coefficients in the simulations were empirically determined from measurements (see Supplementary Information section S7). The repulsive forces between particles were modelled with a spring and damper. To determine parameters for these forces, a grid search was conducted using simulations of an experiment involving five particles in a row, and the parameters that best replicated the experimental results were chosen. These model parameters were then verified by simulating another physical experiment consisting of an amorphous configuration of ten particles. The centroid path of the simulated particles approximately matches that of the experiment, falling within 10 cm (less than one contracted particle) of the expected path of motion (Supplementary Information section S8, Supplementary Video 5).

It should be noted that the attraction between physical particles occurs at discrete points because the forces act only where the flexible magnetic compartments couple. As a result, the physical particle robots tend to preserve their general shape and are more likely to rotate as they move towards the light source. On the other hand, in the simulation, the attraction between the particles was modelled as a continuous force acting along their outer surfaces, allowing the particle arrangement to be more flexible, whereby they can move along each other's perimeter in lieu of turning. Despite this difference, the simulation still models the behaviour qualitatively, as demonstrated by the verification experiment of ten amorphous particles. Another important assumption is that the environmental signal and sensor fidelity scale proportionally as the number of particles is increased.

Graphical processing units were employed for improved computational performance during simulations. Parallel processing of this dynamic system allowed simulations to run much faster than real-time experiments, with up to two billion particle–particle interactions calculated per second. The simulation environment thus permitted examining the performance of particle robots consisting of >10^4 particles. In each case, the system centroid was calculated to verify that the system moved towards the simulated light source.

In the simulations and experiments conducted as part of this work, the wavelength was set to five times the minimum particle diameter. Consequently, when the robot moved, a wave pattern roughly five particles in length could be discerned. When a fully functioning particle robot is small, consisting of approximately ten particles, this wavelength results in a single full wave of oscillation across the system at any given time, moving at an average speed of 1.24 ± 0.44 mm s^{-1} (or $9.60\% \pm 3.40\%$ of the minimum particle diameter per cycle) when no dead particles are present (Supplementary Information section S9).

Code and data availability
The simulation code and datasets generated during this study are available at https://github.com/richa-batra/ParticleRobotSimulations.git.

31. Strogatz, S. *Sync: The Emerging Science of Spontaneous Order* (Hyperion, New York, 2003).
32. Mirollo, R. E. & Strogatz, S. H. Synchronization of pulse-coupled biological oscillators. *SIAM J. Appl. Math.* **50**, 1645–1662 (1990).
33. Christensen, A. L., O'Grady, R. & Dorigo, M. From fireflies to fault-tolerant swarms of robots. *IEEE Trans. Evol. Comput.* **13**, 754–766 (2009).
34. Perez-Diaz, F., Zillmer, R. & Gross, R. Firefly-inspired synchronization in swarms of mobile agents. In *Proc. 2015 International Conference on Autonomous Agents and Multiagent Systems* 279–286 (International Foundation for Autonomous Agents and Multiagent Systems, 2015).
35. Rubenstein, M., Ahler, C., Hoff, N. & Cabrera, A. Kilobot: a low cost robot with scalable operations designed for collective behaviors. *Robot. Auton. Syst.* **62**, 966–975 (2014).